This article has been accepted for inclusion in a future issue of this journal. Content is final as presented, with the exception of pagination.

Optimization Method for Configuration Set for Field Calibration of Industrial Robot

Ziyi Wang, *Student Member, IEEE*, Lan Qin, Jingcheng Liu, Min Li, and Jun Liu

Abstract*—In the calibration process of industrial robots, selecting the optimal measurement position configuration can improve calibration accuracy. However, existing research on the optimal measurement configurations selection mainly focuses on open-loop measurement methods using laser trackers. The exploration of the optimal measurement configuration selection for closed-loop measurement methods has not been developed to a large extent. This research introduces a measurement configurations selection observability index based on the position difference error equation, as well as an optimization method based on this index. Initially, we establish an error model for the kinematic parameters of industrial robots, which is based on the position difference of measurement configurations. Subsequently, by minimizing the relative error of the measurement, we proposed an observability index, denoted as O_e. Using this index, construct a fitness function and use particle swarm optimization (PSO) algorithm to optimize the selection of robot measurement configuration set. The effectiveness of the proposed optimization method has been demonstrated through experiments conducted on CRP RA07 and JAKA Zu seven robots. The experimental results show that using the observability index O_e to select the optimal configuration set can improve the calibration accuracy of the robot by 25.8% and 37.0%, respectively. The verification experiment using a laser tracker confirms that our optimal configuration set selection method can effectively improve calibration accuracy. This research fills the gap in the selection of optimal measurement configurations for constrained measurement. It is of great significance for field calibration research of robots.

***Index Terms*—Field calibration, industrial robot, kinematics, measurement configuration set optimization.**

I. Introduction

IN recent years, industrial robot have been widely used in industrial production.

As the service life of these robots extends, their positioning errors tend to accumulate [1], [2]. Geometric parameter errors account for 90% of these total positioning errors [3]. To enhance the position accuracy of industrial robots, field calibration is essential. To mitigate the effects of measurement noise on calibration accuracy, measurement configurations that more accurately reflect kinematic parameter errors should be chosen to form the calibration configuration set.

The field calibration of industrial robots mainly adopts open-loop and closed-loop measurement methods. The most accurate measurement method among them is open-loop measurement, such as laser tracker measurement. However, the high cost of equipment poses a significant obstacle for users. Therefore, robot users usually adopt closed-loop measurement methods. Common closed-loop measurement methods include point constrained measurement [4], [5], line constrained measurement [6], [7], and area constrained measurement [8], [9]. Among them, the point-to-point calibration method first proposed by Bennett and Hollerbach [10] is the most representative field calibration method.

Although this method is cost-effective in calibrating equipment, it heavily relies on manual calibration by users. Due to human factors, this dependence can significantly affect measurement accuracy, so calibration effectiveness cannot be guaranteed. To address this issue, we have developed an industrial robot calibration system based on a single position sensitive detector (PSD) [11]. The system uses a point light source matrix to determine the position of the robot end effector at the PSD projection position, and quantifies the position error during point constraint measurement. However, during the measurement process, we discovered that the selection of measurement configurations significantly impacts the calibration results.

The measurement configuration set is a collection of measurement pose configurations used for robot calibration. By selecting different measurement poses to form a configuration set, the accuracy of robot calibration can be changed. The optimal selection of a measurement configuration set typically involves determining the observability index. This index measures the impact of robot measurement configurations on calibration results. The commonly used observability indices are usually a criterion about singular values of identification Jacobian matrix. There are five types: Borm and Meng [12] proposed that the product of all nonzero singular values of the identification Jacobian matrix can reflect the volume of an ellipsoid, using the volume of the error ellipsoid as a criterion, termed as O_1. Driels and Pathre [13] used the reciprocal of the condition number as a criterion, expressed as O_2. Nahivi et al. [14] proposed the minimum singular value of the Jacobian

Received 13 May 2024; revised 6 August 2024 and 8 September 2024; accepted 20 September 2024. This work was supported by the Natural Science Foundation Project of China under Grant 52175494.
(Corresponding author: Jun Liu.)

The authors are with the Key Laboratory of Optoelectronic Technology and Systems of Ministry of Education, College of Optoelectronic Engineering, Chongqing University, Chongqing 400044, China (e-mail: ziyi@cqu.edu.cn; qinlan@cqu.edu.cn; jcliu@cqu.edu.cn; limin780815@cqu.edu.cn; junliu@cqu.edu.cn).
Digital Object Identifier 10.1109/TIE.2024.3472289

0278-0046 © 2024 IEEE. Personal use is permitted, but republication/redistribution requires IEEE permission.
See https://www.ieee.org/publications/rights/index.html for more information.

Authorized licensed use limited to: SHANDONG UNIVERSITY. Downloaded on January 06,2025 at 08:09:21 UTC from IEEE Xplore. Restrictions apply.

This article has been accepted for inclusion in a future issue of this journal. Content is final as presented, with the exception of pagination.

matrix as an observability index, denoted as O_3. Nahivi and Hollerbach [15] further proposed a criterion as O_4, based on the product of the minimum singular value and the reciprocal of the condition number. Sun and Hollerbach [16] proposed the reciprocal of the sum of the reciprocals of nonzero singular values as the criterion, expressed as O_5. In addition to these widely accepted observability indices, scholars have also proposed new measurement configuration selection methods in recent years. Wang et al. [17] proposed a more universal observability index and validated its effectiveness on a surgical robot. Deng et al. [18] used the sequential floating forward selection (SFFS) algorithm to optimize the observability index of gravity model parameters, achieving the optimization selection of stiffness model measurement configuration. Ye and Wu [19] used the reciprocal of the expected root mean square of the residual square as an observability metric and validated the effectiveness of the residual index using a 5-degree-of-freedom hybrid robot. Wu et al. [20] used weighted traces of correlated covariance matrices to construct observability index, reducing the impact of measurement noise on recognition results. However, current research on the optimal selection of measurement configuration set for industrial robots is generally based on open-loop measurement methods, exemplified by the use of laser trackers for verification. The measurement configurations used in these researches are selected in a larger workspace, and due to the use of laser trackers to establish the robot's benchmark, there is no coupling relationship between the measurement configurations, which can intuitively reflect the robot's position errors. The configuration optimization of closed-loop measurement methods, represented by point-to-point, differs from that of open-loop measurement methods. The measurement configurations that can be selected by closed-loop measurement methods are limited by constraint conditions, making it challenging to directly establish the robot's benchmark. Usually, the position difference error between measurement configurations is used for parameter identification, resulting in coupling relationships between measurement configurations. Current research on measurement configuration optimization for closed-loop measurement methods is almost nonexistent.

To address the above issues, this research proposed a measurement configuration observability index based on point constrained measurement method and an optimal configuration selection method based on this index, which considers the characteristics of the differential position equation under point constrained measurement method. Experiments were conducted leveraging an optimization algorithm to ascertain the optimal measurement configuration set for industrial robots under this index. The experimental results demonstrated that the calibration accuracy of the robot was significantly improved after the optimal configuration was selected.

The remainder of this article is structured as follows: Section II introduces the measurement principles and the modeling of kinematic error parameters in robots, as well as the methods for their identification. Section III presents the concept of the observability index, which is based on the differential error equation, along with the method for optimizing the measurement configuration set using the PSO algorithm. Section IV verifies the proposed methods through experimentation. Finally, Section V recaps the primary accomplishments and contributions of this research.

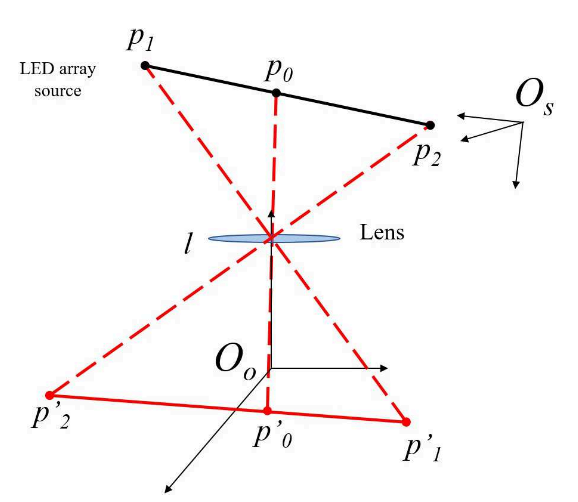


Fig. 1. Geometric model of "three-point measurement method."

II. Calibration Method for Kinematic Model

Robot calibration technology generally consists of four steps: modeling, measurement, identification, and compensation. Among them, the measurement and identification part has always been the difficult points in field calibration research of industrial robot.

A. Measurement Method

Due to the high price of laser trackers, the industry is trying to use other less expensive methods to measure robots. The measurement device used in this article is a self-developed 3D spatial position measurement device based on multipoint imaging detection using a single PSD [11]. The point source matrix of the probe is projected onto the PSD sensor through a single lens assembly, and the target point position is calculated by analyzing the projection information.The principle of the measurement device is shown in Fig. 1.

The coordinate system $\{O_0\}$ refers to the PSD sensing plane, whose origin is the PSD center point. The coordinate system $\{O_s\}$ represents the point light source matrix coordinate system, with point light sources numbered p_0, p_1, and p_2, and their geometric relationships remain equidistant and collinear. p'_i is the projection of p_i on the photosensitive surface of the sensor, where $i = 0,1,2$. In the model shown in Fig. 1, the distance between the lens and PSD is the focal length of the lens, and its geometric coordinates can be expressed as $l = [0, 0, f]$.

The location of the projection point can be measured by a sensor, that is, the coordinates of p'_i can be expressed as $p'_i = [x_i, y_i, 0]$, where $i = 0,1,2$. According to the principle of pinhole imaging, p_i, l, and p'_i are on the same straight line. Constructing a vector starting from l, we can obtain

$$\overrightarrow{lp_i} = k_i \cdot \overrightarrow{lp'_i}. \tag{1}$$

Authorized licensed use limited to: SHANDONG UNIVERSITY. Downloaded on January 06,2025 at 08:09:21 UTC from IEEE Xplore. Restrictions apply.

This article has been accepted for inclusion in a future issue of this journal. Content is final as presented, with the exception of pagination.

The spatial geometric position relationships of p_0, p_1, and p_2 constitutes geometric constraints on vector $\overrightarrow{lp_i}$, which can be formulated as

$$\begin{aligned} \left\|\overrightarrow{lp_1} - \overrightarrow{lp_0}\right\| &= \mathrm{d} \\ \left\|\overrightarrow{lp_0} - \overrightarrow{lp_2}\right\| &= \mathrm{d} \\ \overrightarrow{lp_1} - \overrightarrow{lp_0} &= \overrightarrow{lp_0} - \overrightarrow{lp_2} \end{aligned} \tag{2}$$

where d is the length of p_0p_1 and p_0p_2.

By substituting the expression of $\overrightarrow{lp_i}$, we can obtain

$$\begin{aligned} (k_1x_1 - k_0x_0)^2 + (k_1y_1 - k_0y_0)^2 &= \mathrm{d}^2 \\ (k_2x_2 - k_0x_0)^2 + (k_2y_2 - k_0y_0)^2 &= \mathrm{d}^2 \\ k_1x_1 + k_2x_2 &= 2 \cdot k_0x_0 \\ k_1y_1 + k_2y_2 &= 2 \cdot k_0y_0 \\ k_1 + k_2 &= 2 \cdot k_0. \end{aligned} \tag{3}$$

In this equation set, there are three unknowns, k_0, k_1, and k_2, and three equations, so it can be solved. By solving the value of k_0, the value of the displacement vector ${}^0T_s$ at this point can be obtained, which can be directly expressed as

$${}^0T_s = [k_0x_0, k_0y_0, (1 - k_0)f]. \tag{4}$$

The position of p_0 in the coordinate system of the measuring device can be solved.

B. Error Model Based on D-H Method

The first step in establishing a robot error model is to determine the kinematic model used by the robot. The D-H method is the most common method for describing the relationship between links, and the robot model constructed using the D-H method is widely used in industrial robot controllers.

In the D-H method, each link has four parameters, namely, the length of connecting rod a, torsion angle of connecting rod α, joint distance d, and joint angle θ.

The serial robot composed of multiple connecting rods can be expressed as

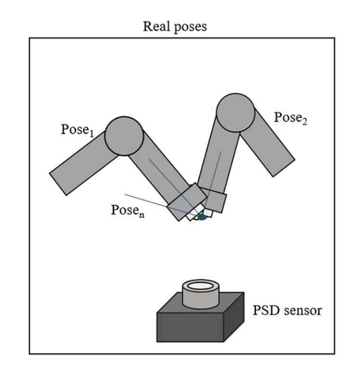
$${}^0T_n = {}^0T_1\,{}^1T_2 \ldots {}^{n-1}\ T_n = \prod_{i=1}^{n} {}^{i-1}T_i \tag{5}$$

where ${}^{i-1}T_i$ is the homogeneous transformation matrix from the $(i-1)$th link to the ith link, and n is the number of links the robot has.

The robot used in this article is a six-axis industrial robot CRP RA-07. This robot is a classic 6R robot, which has six rotational axes. The robot requires the addition of tools to complete specific tasks, which introduces additional coordinate transformation relationships for the robot. Let the calibration tool matrix be ${}^nT_{\text{tool}}$, then its transformation matrix can be expressed as

$${}^nT_{\text{tool}} = \begin{bmatrix} {}^nR_{\text{tool}} & {}^nP_{\text{tool}} \\ 0 & 1 \end{bmatrix} \tag{6}$$

where ${}^nR_{\text{tool}}$ is the tool rotation matrix, and since the calibration tool does not need to consider pose transformation, it is set to be the identity matrix. ${}^nP_{\text{tool}}$ is a tool for translating matrix, ${}^nP_{\text{tool}} = [x_{\text{tool}}, y_{\text{tool}}, z_{\text{tool}}]^T$. ${}^nT_{\text{tool}}$ shows the transformation from end of robot links to tool centre position (TCP).



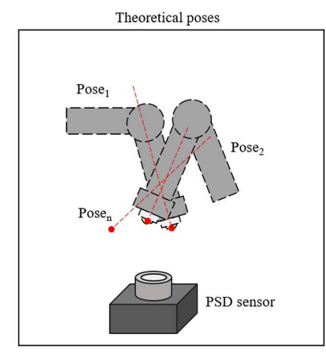


Fig. 2. Measurement method for robot TCP position.

The homogeneous transformation matrix from the base coordinate system $\{O_0\}$ to the tool coordinate system $\{O_{\text{tool}}\}$ is

$${}^0T_{\text{tool}} = {}^0T_1\,{}^1T_2 \ldots {}^5\ T_6\,{}^6T_{\text{tool}}. \tag{7}$$

The model ${}^0T_{\text{tool}}$ consists of six links and a tool, which involves seven coordinate transformations. Therefore, the position error e_p is also composed of parameter errors in the homogeneous transformation matrix, which can be expressed as

$$e_p = [e_x, e_y, e_z]^T = f(e_{a_i}, e_{\alpha_i}, e_{d_i}, e_{\theta_i}, e_{x_{\text{tool}}}, e_{y_{\text{tool}}}, e_{z_{\text{tool}}}) \tag{8}$$

where e_p is the difference between the theoretical position and the measured position, e_{a_i}, e_{α_i}, e_{d_i}, e_{θ_i}, $e_{x_{\text{tool}}}$, $e_{y_{\text{tool}}}$, $e_{z_{\text{tool}}}$ are the errors of the parameters in each link, $i = 1, \ldots, 6$.

According to the differential principle, the transfer of D-H parameters in various directions can be expressed as follows:

$$\begin{aligned} e_{p_x} &= \frac{\partial f_x}{\partial a_1} e_{a_1} + \frac{\partial f_x}{\partial a_2} e_{a_2} + \cdots + \frac{\partial f_x}{\partial z_{\text{tool}}} e_{z_{\text{tool}}} \\ e_{p_y} &= \frac{\partial f_y}{\partial a_1} e_{a_1} + \frac{\partial f_y}{\partial a_2} e_{a_2} + \cdots + \frac{\partial f_y}{\partial z_{\text{tool}}} e_{z_{\text{tool}}} \\ e_{p_z} &= \frac{\partial f_z}{\partial a_1} e_{a_1} + \frac{\partial f_z}{\partial a_2} e_{a_2} + \cdots + \frac{\partial f_z}{\partial z_{\text{tool}}} e_{z_{\text{tool}}}. \end{aligned} \tag{9}$$

If the calibration includes N measurement configurations, let the theoretical position be P and the actual position be P', then it can be represented as a matrix as

$$\Delta P_k = J_k \eta_k \tag{10}$$

where ΔP_k is the position error, $\Delta P_k = P' - P = [e_{p_{x1}}, e_{p_{y1}}, e_{p_{z1}}, e_{p_{x2}}, \ldots, e_{p_{xN}}, e_{p_{yN}}, e_{p_{zN}}]^T$, J_k is the jacobian matrix of kinematic parameters, and η_k is the kinematic parameter vector, $\eta_k = [e_{a_1}, e_{a_2}, \ldots, e_{z_{\text{tool}}}]^T$.

The measurement method based on point constraints can constrain the actual end position of the robot to the center point of the sensor measurement, as shown in Fig. 2. The solid line in the figure represents the position of the robot's end effector during the actual measurement process, and it can be seen that the robot's end effector intersects at a point under point constraints. The dashed line represents the theoretical position, and due to the presence of kinematic parameter errors, the end position calculated through joint angles cannot be converged to

Authorized licensed use limited to: SHANDONG UNIVERSITY. Downloaded on January 06,2025 at 08:09:21 UTC from IEEE Xplore. Restrictions apply.

This article has been accepted for inclusion in a future issue of this journal. Content is final as presented, with the exception of pagination.

the same point. The advantage of this approach is that the actual measurement accuracy of the robot is linked to the repeatability accuracy of the measurement device, which can achieve high measurement accuracy. The disadvantage is that the closed-loop adjustment of the robot end position is required during the measurement process, which is slower than the open-loop measurement method based on theoretical model point constraints to generate poses.

When using a laser tracker for calibration, a circle point analysis (CPA) method is required to determine the coordinate transformation relationship between the laser tracker and the robot base [21]. However, in the field calibration method based on the single PSD, the transformation relationship between the robot base coordinate system and the sensor coordinate system cannot be directly obtained through measurement. Therefore, the position error differential method is used to identify the robot error parameters during the identification process.

C. Method for Identifying Kinematic Model Parameters Based on Differential Position Error

Equation (10) shows how the kinematic model parameter error is converted into a position error. Generally, we only need to divide the position error matrix ΔP_k by the Jacobian matrix J_k (left division) to obtain the value of the parameter error matrix η_k, which is $\eta_k = J_k^{-1}\Delta P_k$. As a nonsquare matrix, the inverse of the J_k matrix cannot be directly calculated. To ensure that the rank of the matrix is full, the system of equations is usually overdetermined, so an optimization method is needed to solve the parameter error matrix η_k.

Generally speaking, the least squares method can solve this problem by calculating $\eta_k = (J_k^T J_k)^{-1} J_k^T \cdot \Delta P_k$. However, for a nonlinear system such as industrial robot, a corresponding nonlinear optimization method is required to optimize the solution process.

The most common parameter identification algorithm for solving industrial robot parameters is the Levenberg-Marquardt (LM) algorithm, which combines the advantages of Newton's method and gradient descent method. Its iterative expression is usually as follows:

$$\begin{aligned} \Delta\eta_{ki+1} &= (J_k^T J_k + \lambda_i I)^{-1} J_k^T \cdot \Delta P_k \\ \eta_{ki+1} &= \eta_{ki} - \Delta\eta_{ki+1} \end{aligned} \tag{11}$$

where i is the number of iterations, λ_i is the damping factor, whose value is determined by the convergence of the error.

Unlike laser trackers, industrial robot field calibration equipment based on a single PSD is difficult to determine the positional transformation relationship between the sensor coordinate system and the base coordinate system. Therefore, we need to use a differential identification algorithm for parameter.

Equation (10) can express as

$$\begin{bmatrix} \Delta p_{k1} \\ \Delta p_{k2} \\ \cdots \\ \Delta p_{kN} \end{bmatrix} = \begin{bmatrix} \Delta j_{k1} \\ \Delta j_{k2} \\ \cdots \\ \Delta j_{kN} \end{bmatrix} \cdot \eta_k \tag{12}$$

where Δj_{ki} is the Jacobian matrix of the ith pose, and Δp_{ki} is the position error of the ith pose, which are the sub elements of J_k and ΔP_k, respectively. The position error Δp_{ki} is composed of the position error Δp_{pi} from the robot end to the sensor coordinate and the position error Δp_s from the sensor to the base coordinate, i.e., $\Delta p_{ki} = \Delta p_{pi} + \Delta p_s$. Usually, Δp_s needs to be obtained through measurement. However, when differentiating the (12), the following equation can be obtained as:

$$\begin{bmatrix} \Delta p_{k1} - \Delta p_{k2} \\ \Delta p_{k2} - \Delta p_{k3} \\ \cdots \\ \Delta p_{kN-1} - \Delta p_{kN} \end{bmatrix} = \begin{bmatrix} \Delta j_{k1} - \Delta j_{k2} \\ \Delta j_{k2} - \Delta j_{k3} \\ \cdots \\ \Delta j_{kN-1} - \Delta j_{kN} \end{bmatrix} \cdot \eta_k. \tag{13}$$

Substituting $\Delta p_{ki} = \Delta p_{pi} + \Delta p_s$, we have

$$\begin{bmatrix} \Delta p_{p1} - \Delta p_{p2} \\ \Delta p_{p2} - \Delta p_{p3} \\ \cdots \\ \Delta p_{pN-1} - \Delta p_{pN} \end{bmatrix} = \begin{bmatrix} \Delta j_{k1} - \Delta j_{k2} \\ \Delta j_{k2} - \Delta j_{k3} \\ \cdots \\ \Delta j_{kN-1} - \Delta j_{kN} \end{bmatrix} \cdot \eta_k. \tag{14}$$

Therefore, parameter identification can be performed without measuring the position of the sensor to the robot base coordinate by using the (14), which can be written as

$$\Delta P_k^* = J_k^* \eta_k. \tag{15}$$

This equation is still applicable to the LM algorithm. In this article, its iterative expression is as

$$\begin{aligned} \Delta\eta_{ki+1} &= (J_k^{*T} J_k^* + \lambda_i I)^{-1} J_k^{*T} \cdot \Delta P_k^* \\ \eta_{ki+1} &= \eta_{ki} - \Delta\eta_{ki+1}. \end{aligned} \tag{16}$$

III. Optimal Measurement Configurations Selection Method

Choosing the optimal measurement configurations can reduce measurement noise interference and improve the calibration accuracy of robots. Generally speaking, optimal measurement configurations selection should consider two indispensable aspects, namely observability index and search algorithms.

A. Observability Index Considering Differential Position Error

Due to the limitation of the working space position at the end of the field calibration measurement method used in this article, it is more necessary to optimize the measurement pose configuration.

The five widely used observability indices are all defined based on the singular values of the Jacobian matrix of the identified parameters. Through singular value decomposition (SVD), the Jacobian matrix of the identified parameters can be expressed as

$$J_k = U \Sigma V^T \tag{17}$$

where U and V are the orthogonal matrices, and Σ is a diagonal matrix. Since the calibration equation set is overdetermined, the Jacobian matrix J_k is not a square matrix. Therefore, when the number of identified parameters is L, Σ can be expressed as

$$\Sigma = \begin{bmatrix} \Lambda \\ 0 \end{bmatrix}, \Lambda = \mathrm{diag}(\sigma_1, \sigma_2, \ldots, \sigma_L) \tag{18}$$

Authorized licensed use limited to: SHANDONG UNIVERSITY. Downloaded on January 06,2025 at 08:09:21 UTC from IEEE Xplore. Restrictions apply.

This article has been accepted for inclusion in a future issue of this journal. Content is final as presented, with the exception of pagination.

where $\text{diag}(\sigma_1, \sigma_2, \ldots, \sigma_L)$ denotes a diagonal matrix, and σ_i is the singular value of the Jacobian matrix J_k, $i = 1, \ldots, L$.

According to the theory proposed by Borm and Meng [12], assuming that there are robot parameter errors in a unit radius sphere, a multidimensional space hyperellipsoid can be generated. This ellipsoid can be seen as the robot end-effector position error caused by parameter errors, and its mapping principle is the same as the transformation of a unit circle in a 2-D plane into an ellipse. The length of each principal axis radius of the ellipsoid is the singular value of the identification matrix. The observability index O_1 is the geometric mean of all singular values. Maximizing the geometric mean of singular values increases the sensitivity of position errors relative to kinematic parameter errors, that is, reduces the interference caused by measurement errors. O_1 can be expressed as

$$O_1 = \frac{(\sigma_1 \sigma_2 \ldots \sigma_l)^{1/L}}{\sqrt{M}} \tag{19}$$

where L is the number of singular values, and M is the number of measurements.

However, in (15), the position error ΔP_k^* obtained by the position differential method is not the difference between the actual position of the measurement configuration and the actual position, but the position difference between one measurement configuration and the previous measurement configuration. The differential error matrix does not represent the first-order relationship of the robot's true position. Therefore, the singular values of the differential Jacobian matrix J_k^* are no longer the sensitivity of the parameter error itself, although they have an impact on sensitivity. Maximizing the singular value ellipsoid will result in incorrect optimal solutions. We need to propose a new observation metric to indicate the characteristics of the calibration configuration set.

It can be found here that in traditional parameter identification methods, the position error ΔP_k is constant, and ΔP_k is fixed after the measurement is completed, and the optimization process cannot be considered. In the identification based on the differential parameter error equation, the difference ΔP_k^* between the position errors of the end-effector can be changed through pose optimization.

Due to the inevitable noise caused by the instrument, which is not related to the measurement configuration, and the noise cannot be directly measured, if the instrument measurement error is considered as a constant value, and if the measurement error of Δp_{ki} is set to $\pm\sigma_P$, and the true value of Δp_{ki} is Δp_{kti}, then

$$\Delta p_{ki} = \Delta p_{kti} \pm \sigma_P. \tag{20}$$

In (15), ΔP_k^* is the difference between the end position errors in different configurations. According to the definition, we have

$$\Delta p_{ki}^* = \Delta p_{ki} - \Delta p_{ki+1} = \Delta p_{kti} - \Delta p_{kti+1} \pm 2\sigma_P \tag{21}$$

where Δp_{ki}^* is the difference of position errors, $i = 1, \ldots, N-1$. We can define the relative error of Δp_{ki}^* as

$$\delta \Delta p_{ki}^* = \frac{2\sigma_P}{|\Delta p_{kti} - \Delta p_{kti+1}| + 2\sigma_P}. \tag{22}$$

If the value of $|\Delta p_{kti} - \Delta p_{kti+1}|$ is smaller, it represents a lower relative accuracy and greater interference from measurement errors. As a consequence, the larger the value of $|\Delta p_{ki} - \Delta p_{ki+1}|$, the higher the relative accuracy of Δp_{ki}^*. To suppress the impact of noise on error identification, it is necessary to consider the characteristics of the position error differential vector in the observability index. But if the observability index only considers $\delta \Delta p_{ki}^*$, the use of this observability index for configuration set optimization may result in pose selections slip to several poses that can achieve the maximum local difference, which may lead to too many repeated poses in the configuration set. Excessive repetition of poses can result in the Jacobian matrix of the configuration set not having sufficient rank and poor parameter identification ability. Therefore, to ensure the full rank of the parameter Jacobian matrix, it is necessary to use singular values in the observation index to comprehensively optimize pose selection. Considering that matrices with low rank inevitably have singular values of zero, the method of multiplying singular values can be used for discrimination.

Therefore, based on the differential characteristics of the parameter identification equation in field calibration, an optimized observability index O_e can be proposed as

$$O_e = \frac{(\sigma_1 \sigma_2 \ldots \sigma_l)^{1/L}}{\sqrt{L}} \cdot \frac{(\Delta p_{k1} \Delta p_{k2} \ldots \Delta p_{kN-1})^{1/N-1}}{\sqrt{N-1}} \tag{23}$$

where σ_i is the singular value of the differential Jacobian matrix, $i = 1, \ldots, L$, L is the number of calibration parameters; Δp_{ki} is the differential value of the measurement position error, $i = 1, \ldots, N-1$, N is the number of measurement configurations.

By definition, the value of O_e is the geometric mean of the measured configuration's position difference values multiplied by an observability index O_1, which considers the characteristics of both J_k^* and ΔP_k^*. Optimizing the measurement configuration set is to maximize the differential of the measured positions of the configuration, and improve the identification characteristics of the parameters by expanding the volume of the hyperellipsoid of the position error difference in the differential identification equation. This observability index also considers the singular values of the Jacobian matrix, as the Jacobian matrix is an important coefficient that cannot be ignored in the identification equation. Adding the singular value index of the Jacobian matrix can prevent the phenomenon of over-concentration in the configuration set during the optimization process due to the uneven distribution of the measurement data set, and improve the stability of the optimization process.

According to the definition, the value of O_e is the geometric mean of the position difference values of the measurement configuration multiplied by an observability index O_1. The O_1 here is used to ensure that the Jacobian matrix is full rank. Using this observability index to optimize the measurement configuration set is to minimize the relative error of differential measurements in the configuration set.

Authorized licensed use limited to: SHANDONG UNIVERSITY. Downloaded on January 06,2025 at 08:09:21 UTC from IEEE Xplore. Restrictions apply.

This article has been accepted for inclusion in a future issue of this journal. Content is final as presented, with the exception of pagination.

B. Optimization Method for Pose Configuration Based on Particle Swarm Optimization (PSO)

Particle swarm optimization algorithm has excellent performance in solving nonlinear optimization problems and is one of the commonly used algorithms. Its principle is to set multiple particles that move in the optimization parameter space, construct two basic equations of position and velocity to drive each particle to move to optimize the objective function. The position and velocity of each particle are evolved by the following two equations:

$$V_i^{t+1} = \omega^t V_i^t + c_1 R_{i1}^t (G_i^t - P_i^t) + c_2 R_{i2}^t (G_g^t - P_i^t)$$
$$P_{i+1}^t = P_i^t + V_i^{t+1} \quad (24)$$

where c_1 and c_2 are the cognitive and social learning factors of the particle, respectively, G_i^t and G_g^t represent the individual and group optimal positions as of time t, respectively. R_{i1}^t and R_{i2}^t represent random numbers, ω^t represents the inertia weight.

The traditional PSO algorithm is suitable for processing problems in continuous parameter spaces, but in the problem of pose optimization, the optimized parameters are a discrete set of poses with a specific number of poses, which requires us to improve some of the PSO algorithms. The algorithm flow is mainly includes four steps:

1) Encoding the alternative measurement poses. Unlike the measurement pose when using a laser tracker for calibration, the field calibration measurement pose is usually composed of a series of poses with the TCP ends fixed at the same point. These poses are usually evenly divided according to the pose angles in space, and the individual poses are sequentially encoded according to the spatial order.
2) Initialize PSO parameters. The most important parameter of PSO is to determine the initial state of the particles. Generally, the position and velocity of the particles need to be randomly generated. In field calibration, the initial position can be set to a uniformly distributed initial pose configuration set in space, and the velocity is generated according to a random function.
3) Determine the fitness function. According to the observability metric mentioned earlier, a fitness function is constructed. The purpose of the fitness function is to return a value reflecting the size of the observability index based on the input configuration set.
4) Iteration position and velocity equation. Iterate the particle state according to the position and velocity equations, update the optimal parameters of the particles, stop iteration when the particle swarm reaches the termination condition or the number of iterations reaches the set value, and output an optimal result. If there are more than one point configuration for the position (multiple points in the space are selected for optimization), the optimization space needs to be divided to limit the range of activity of the particles, ensuring that the configuration set positions corresponding to the particles are all located on the same target point (due to the difficulty of expanding the measurement range using the leap-frog method, and the accuracy will be severely reduced, so the geometric relationship between points cannot be calculated).

TABLE I
D-H PARAMETERS OF CRP RA07 ROBOT

i	a (mm)	d (mm)	α (rad)	θ (rad)
1	40	0	−1.5708	0
2	335	0	0	0
3	40	0	−1.5708	0
4	0	335	1.5708	0
5	0	0	−1.5708	0
6	0	89	0	0

TABLE II
TOOL COORDINATE PARAMETERS

x_{tool} (mm)	y_{tool} (mm)	z_{tool} (mm)
120	0	35

IV. VERIFY CONFIGURATION SET OPTIMIZATION METHOD

To demonstrate the feasibility of the calibration method, prototype experiment and validation experiment need to be conducted. Taking the RA07 robot from CRP as the research object, its kinematic model parameters are shown in Table I, and the tool coordinate parameters are shown in Table II.

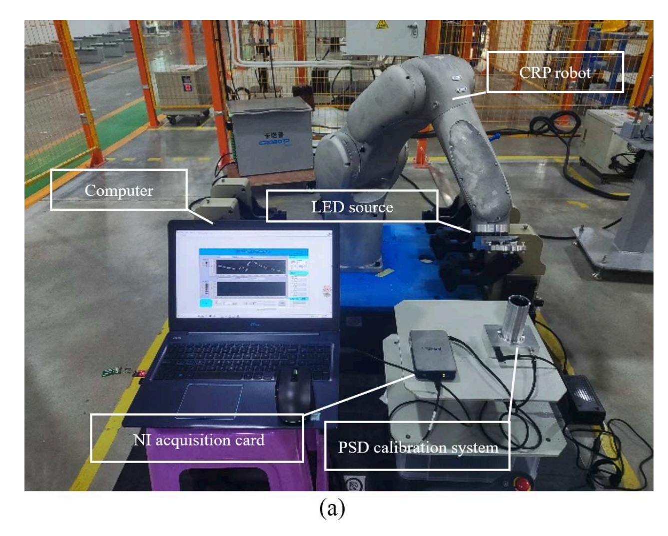
In the structure of robot, the influence of different parameter errors on the final position error is the same for certain different linkages, so we need to eliminate some linearly related parameters. After removing all redundant parameters, we can identify a total of 20 parameters, namely a_1 to a_5, d_3 to d_5, α_1 to α_5, θ_2 to θ_5, as well as x_{tool}, y_{tool}, z_{tool}. Not all calibrated kinematic parameters can be modified by the controller, so error compensation is performed by compensating the joint coordinates in the robot control commands [22].

A. Experimental Verification of Calibration Method Based on Position Difference Index

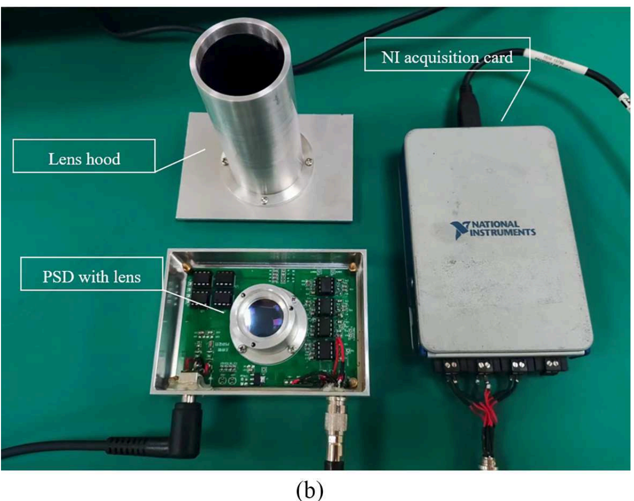
To verify the effectiveness of the method through experiments, we calibrated the robot using different optimization methods based on the single PSD industrial robot calibration system, and verified the calibration results of the robot using a laser tracker system. The single PSD calibration system is shown in Fig. 3, the NI acquisition card, whose model is NI-9215, used to collect the output signal of the PSD sensor box. The PSD sensor model is the S1880 of Hamamatsu, with a resolution of 1.5 μm, and the overall repeatability of the sensor can reach within 20 μm. The light source probe uses the most sensitive red visible LED of PSD as the light source, with a wavelength of 630 nm. The model of six-axis robot is CRP RA07.

Authorized licensed use limited to: SHANDONG UNIVERSITY. Downloaded on January 06,2025 at 08:09:21 UTC from IEEE Xplore. Restrictions apply.

This article has been accepted for inclusion in a future issue of this journal. Content is final as presented, with the exception of pagination.



(a)



(b)

Fig. 3. Calibration results in different configuration set optimization methods. (a) RA07 robot and calibration device. (b) Components of PSD calibration system.

To test the improvement effect of optimizing the measured pose configuration on the calibration result in field calibration using the observability index O_e, a kinematic parameter calibration experiment was conducted on an uncalibrated robot. The light source probe is mounted on the end of the robot, and the PSD sensing box is placed at a certain location in the robot workspace. Since the robot TCP actual position is used as a constraint condition, the sensor pose problem can be ignored. Around the sensor center point of this location, the robot is operated to generate multiple measurement configurations, and these configurations are used as candidate configurations for optimization and parameter identification. The experiment selected measurement points in three directions: the front, left front, and right front of the robot. Each point selected eight poses, totaling 24 poses for parameter identification.

This experiment used observability index O_e and observability index O_1 to select the optimal measurement configuration for the robot. To verify the effectiveness of the observability index, the uniformly spaced selected configuration set is used as a reference for not selecting the optimal measurement configuration.

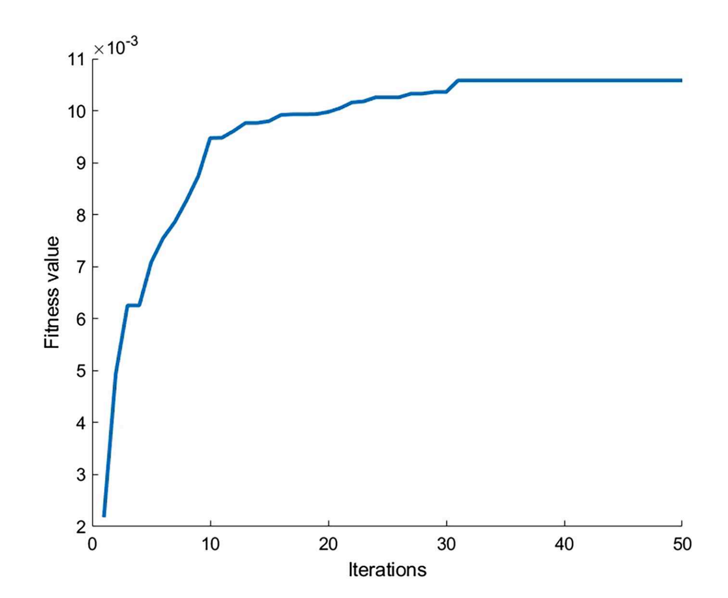


Fig. 4. Value of O_e in the iteration of PSO algorithm.

The results of the observability index O_e in the iteration of the PSO algorithm as shown in Fig. 4. The algorithm sets up 400 particles, with cognitive and social learning factors c_1 and c_2 set to 0.7 and inert weight w set to 0.75, while limiting the maximum particle velocity to 6. This configuration enables particles to quickly search for local optimal values while also considering overall trends during the optimization process. As can be seen from the figure, thanks to the number of particles, the algorithm converged to a stable local optimal value with very few iterations. The algorithm terminated in the 50th iteration, and the observability index changed from the initial 0.0022 to 0.0106. The total memory occupied by the program is 1408 Kb, and it takes about 8 s to execute one iteration. After 35 iterations, it has basically reached the local optimal solution. Therefore, the number of iterations is limited to 50, and our algorithm will take approximately 6 min to optimize.

The kinematic parameter errors of the robot were calculated by the host computer (as shown in Tables I and II), and the compensation errors were compensated to the robot model to obtain the pre- and post-calibration position errors. The calibration effect of the system was demonstrated by comparing the pre- and post-calibration position errors, as shown in Fig. 5.

The comprehensive positioning error before and after calibration is shown in Table III. It can be seen that the average robot error before calibration is 1.418 mm, with a maximum value of 2.771 mm. After using the configuration set optimized by the observability index O_e, the average robot error is 0.190 mm, with a maximum value of 0.366 mm. After using the configuration set optimized by the observability index O_1, the average robot error is 0.239 mm, with a maximum value of 0.473 mm. After using the configuration set without optimization, the average robot error is 0.256 mm, with a maximum value of 0.497 mm. The results show that the average error after calibration using an unoptimized configuration set decreases

Authorized licensed use limited to: SHANDONG UNIVERSITY. Downloaded on January 06,2025 at 08:09:21 UTC from IEEE Xplore. Restrictions apply.

This article has been accepted for inclusion in a future issue of this journal. Content is final as presented, with the exception of pagination.

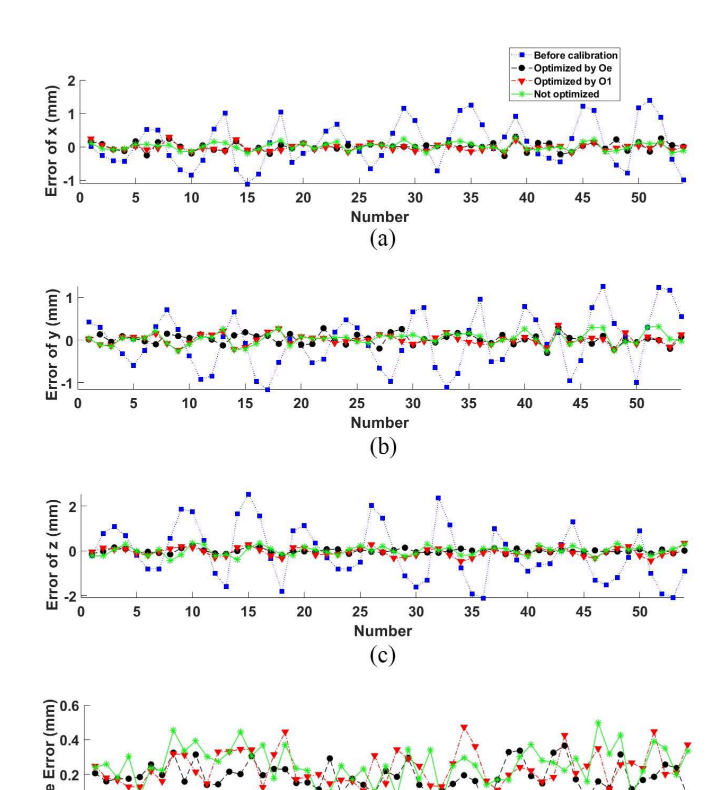


Fig. 5. Calibration results in different configuration set optimization methods. (a) Different optimization methods errors of *x*. (b) Different optimization methods errors of *y*. (c) Different optimization methods errors of *z*. (d) Comparison of results in different optimization methods.

TABLE III
ERRORS OF DIFFERENT OPTIMIZATION METHODS CALIBRATED BY SINGLE PSD INDUSTRIAL ROBOT CALIBRATION SYSTEM

	Before Calibration	Optimized by O_e	Optimized by O_1	Not Optimized
Mean error	1.418 mm	0.190 mm	0.239 mm	0.256 mm
Max error	2.771 mm	0.366 mm	0.473 mm	0.497 mm

to 18.0% of the average error before calibration, while the average error after calibration using an observability index O_e optimized configuration set decreases to 13.4% of the average error after calibration, an increase of 4.6% compared with the unoptimized calibration result.In order to compare with existing technological methods, we applied the definition of observability index O_1 to select the optimal measurement configuration set. The calibration results using the optimal configuration set selected by O_1 showed some improvement compared with the results without selecting the optimal configuration set, but did not show significant improvement in the average and maximum error values. However, the maximum value of the calibration result has been reduced by 13.2% using the observability index O_e. It can be seen that by minimizing the relative error of measurements, the observability index O_e can play a strong role in suppressing the maximum error in the data set of differential position errors.

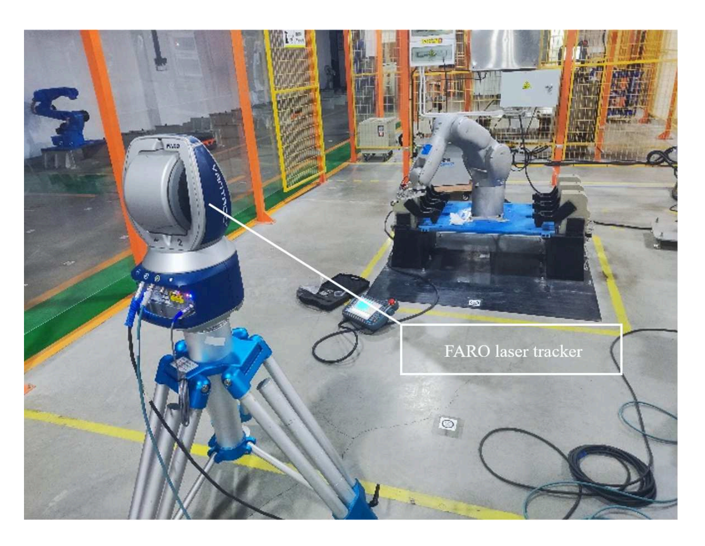


Fig. 6. RA07 robot is calibrated through laser tracker.

B. Verify Calibration Results With Laser Tracker

Using a laser tracker to verify the accuracy of robots calibrated using different methods can verify the effectiveness of the method proposed in this article. The laser tracker system is shown in Fig. 6, The positioning accuracy of FARO Vantage laser tracker is 16 μm. The calibration method we propose is to generate a curve passing near three selected calibration points to represent the working path of the robot. The robot is used to traverse the curve, and 20 points are collected during the process. A reflective ball is mounted on the end of the robot, and the laser tracker is used to measure the position of the robot's end to obtain the position error before and after robot calibration. To compare with existing laser tracker calibration method, we also calibrated the robot using the laser tracker and compared its calibration results with those of our method.

The position error of the robot before and after calibration is shown in Fig. 7 and Table IV. The average error value of the robot after calibration with the configuration set optimized by the observability index O_e is 0.135 mm. The average error value of the robot after calibration with the configuration set optimized by the observability index O_1 is 0.178 mm. Without optimization, the average error value of the robot is 0.342 mm after calibration with the configuration set composed of uniformly selected measurement positions and postures. The mean error value of the calibrated robot is only 0.085 mm when the laser tracker is used to calibrate the robot. The laser tracker verified that the mean and maximum position errors of robots calibrated using the configuration set optimized by the observability index O_e were improved by 60.5% and 65.7% compared with robots calibrated without the optimized configuration set. The results indicate that the observability index O_e can effectively optimize the robot measurement configuration set, enabling it to exhibit better calibration performance. Through the curve, it can be observed that although the calibration result of O_1 is better than

Authorized licensed use limited to: SHANDONG UNIVERSITY. Downloaded on January 06,2025 at 08:09:21 UTC from IEEE Xplore. Restrictions apply.

This article has been accepted for inclusion in a future issue of this journal. Content is final as presented, with the exception of pagination.

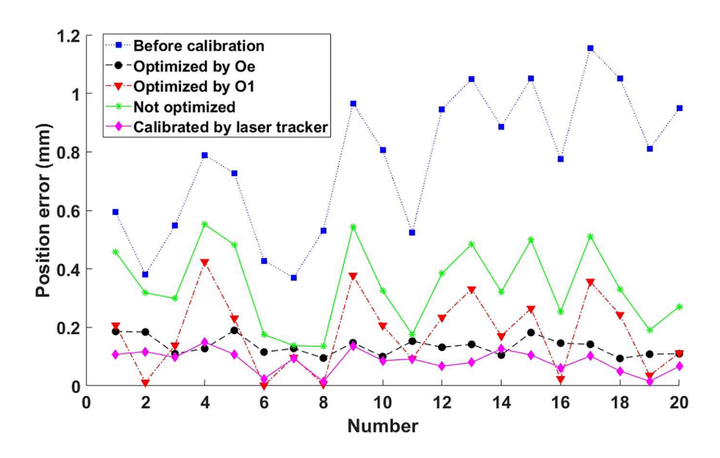


Fig. 7. Calibration results of RA07 with laser tracker.

TABLE IV
VERIFY THE CALIBRATION RESULTS OF VARIOUS OPTIMIZATION METHODS USING A LASER TRACKER

	Before Calibration	Optimized by O_e	Optimized by O_1	Not Optimized	Calibrated by Laser Tracker
Mean error	0.767 mm	0.135 mm	0.178 mm	0.342 mm	0.085 mm
Max error	1.154 mm	0.189 mm	0.424 mm	0.552 mm	0.149 mm

the unoptimized calibration result, the optimized trend of both is the same. In fact, using O_1 to control particles for speed limited exploration can achieve such results, and not limiting particle movement speed can lead to ineffective optimization results. Therefore, according to the verification results of the laser tracker, the experimental conclusion is still valid, and the observability index O_e can effectively optimize the identification results in the constrained field calibration method, especially in the aspect of maximum error suppression. However, it can be seen that in terms of calibration effectiveness, laser trackers have better calibration results than field calibration method, because the laser tracker can perform measurements in a large spatial range, and the more free the measurement space is, the better the fitting effect is.

C. Verify the Effectiveness of the Method on Another Type of Robot

To determine the applicability of the optimal configuration selection method to other types of robots, we conducted experiments using a JAKA Zu 7 collaborative robot similar to CRP RA07, as shown in Fig. 8. The D-H model parameters of the robot are shown in Table V. Considering that the structure of Zu 7 robot is different from that of RA07 robot, after excluding linearly correlated and uncalibrable parameters, a total of 19 parameters need to be calibrated.

The position error of the robot before and after calibration is shown in Fig. 9 and Table VI. Without selecting the optimal calibration configuration set, the average error value of the robot is 0.767 mm. However, after selecting the optimal configuration set for calibration based on the observability index O_e, the average error value decreased to 0.483 mm, an increase of 37.0%. The results indicate that the optimal measurement configuration set selection method proposed in this study is also applicable to the Zu 7 collaborative robot.

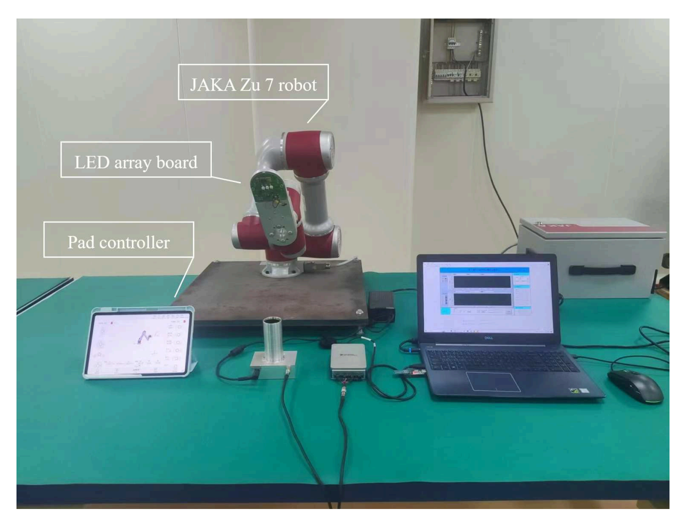


Fig. 8. Zu 7 robot is calibrated through calibration device.

TABLE V
D-H PARAMETERS OF JAKA ZU 7 ROBOT

i	a (mm)	d (mm)	α (rad)	θ (rad)
1	0	0	−1.5708	0
2	360	114.15	0	0
3	303.5	−142.64	0	0
4	0	113.5	−1.5708	0
5	0	113.5	−1.5708	0
6	0	107	0	0

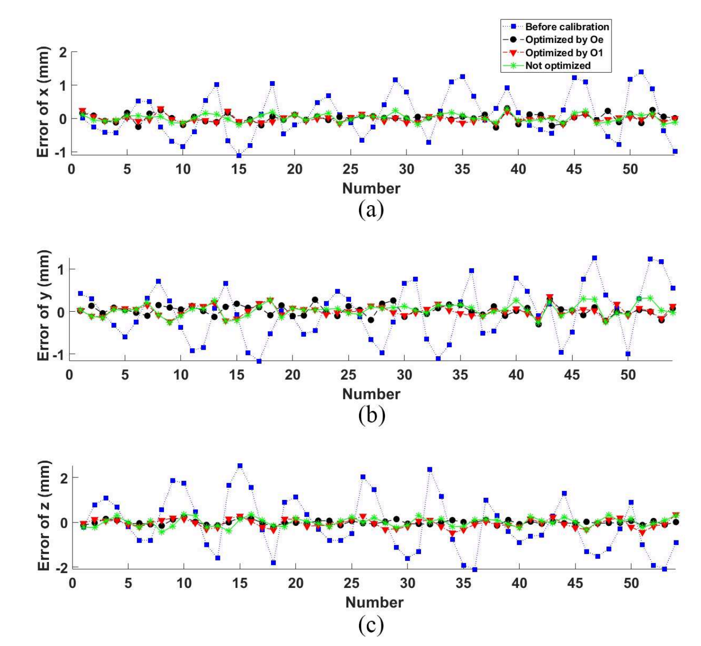
TABLE VI
ERRORS OF ZU 7 COLLABORATIVE ROBOT CALIBRATED BY SINGLE PSD INDUSTRIAL ROBOT CALIBRATION SYSTEM

	Before Calibration	Optimized by O_e	Not Optimized
Mean error	1.925 mm	0.483 mm	0.767 mm
Max error	3.438 mm	1.113 mm	2.242 mm

We conducted measurement experiments on the Zu 7 collaborative robot using a laser tracker to verify the effectiveness of the optimal measurement configuration selection method based on the observability index O_e. The measurement process is the same as parts A and B of Chapter IV. The measurement results are shown in Fig. 10 and Table VII. Compared with the calibration results without selecting the optimal configuration set, the robot calibrated with the selected optimal configuration set reduced its average and maximum position errors by 16.2% and 30.9%, respectively. These results indicate that the optimal measurement configuration set selection method based on observability index O_e is also applicable to other types of robots. However, the degree of accuracy improvement also depends on the type of robot.

Authorized licensed use limited to: SHANDONG UNIVERSITY. Downloaded on January 06,2025 at 08:09:21 UTC from IEEE Xplore. Restrictions apply.

This article has been accepted for inclusion in a future issue of this journal. Content is final as presented, with the exception of pagination.



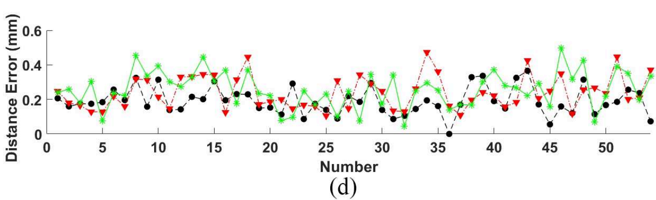


Fig. 9. Calibration results in different configuration set optimization methods. (a) Different optimization methods errors of *x*. (b) Different optimization methods errors of *y*. (c) Different optimization methods errors of *z*. (d) Comparison of results in different optimization methods.

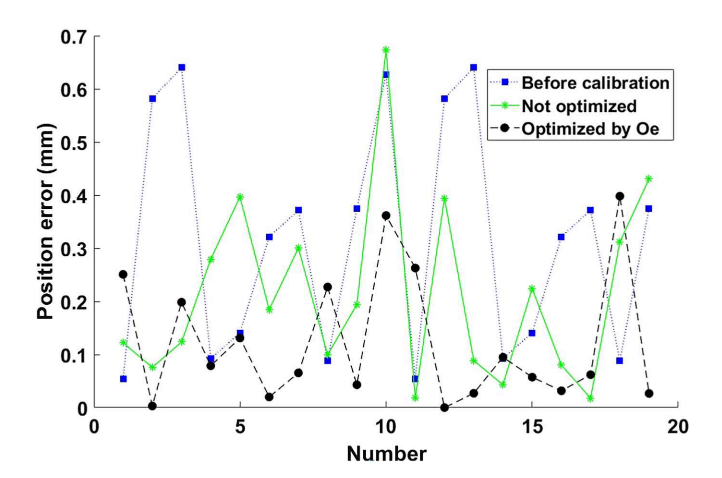


Fig. 10. Calibration results of Zu 7 with laser tracker.

To integrate this method into existing automation control systems, we will develop expandable flanges to integrate sensors into robots without affecting their normal use and tool replacement. We will also develop online automatic calibration control systems and automatic compensation systems to achieve online automatic calibration of industrial robots and maintain their motion accuracy.

TABLE VII
VERIFY THE CALIBRATION RESULTS OF ZU 7 COLLABORATIVE ROBOT USING A LASER TRACKER

	Before Calibration	Optimized by O_e	Not Optimized
Mean error	0.401 mm	0.176 mm	0.210 mm
Max error	0.740 mm	0.674 mm	0.466 mm

V. CONCLUSION

To address the research gap in optimal measurement configurations selection for closed-loop measurement methods in industrial robot calibration, we propose a measurement configurations observability index based on the position difference error equation, along with an optimization algorithm leveraging this index.

The average position error of the CRP RA07 robot, which selected the optimal measurement configurations, decreased from 1.418 to 0.190 mm. Compared with the robot that did not select the optimal measurement configurations, the calibration result improved by 25.8%. The optimal measurement configurations selection method based on observability index O_e effectively suppresses the maximum error, and compared with the calibration results without selecting the optimal measurement configurations, the error is further reduced by 26.4%.

The verification of the laser tracker shows that compared with robot that did not select the optimal measurement configurations, robot that used the observability index O_e to select the optimal measurement configurations reduced the average and maximum position errors after calibration by 60.5% and 65.7%, respectively. This indicates the effectiveness of the observability index O_e in selecting the optimal measurement configurations.

We conducted comparative experiments using the JAKA Zu 7 robot to validate the applicability of the optimal measurement configurations selection method on different robots. The experimental results show that the optimal measurement configurations selected by this method improved the calibration accuracy of the Zu 7 robot by 37.0%. The verification of calibration results using a laser tracker shows that the position accuracy of the robot calibrated with the optimal measurement configurations was improved by 16.2%, which proves that this method is applicable to different types of robots.

The innovation of this research lies in our proposal of an observability index for optimal measurement configuration selection and a method for optimal measurement configuration selection for closed-loop measurement methods. It fills the gap in this field and provides a new solution for improving the calibration accuracy of low-cost robot calibration. Subsequent research can find better solutions by modifying the composition and weights of observability indices, optimizing algorithm types and parameters, etc.

REFERENCES

[1] H. Q. Cao, H. X. Nguyen, T. N.-C. Tran, H. N. Tran, and J. W. Jeon, “A robot calibration method using a neural network based on a butterfly and flower pollination algorithm,” *IEEE Trans. Ind. Electron.*, vol. 69, no. 4, pp. 3865–3875, Apr. 2022.

Authorized licensed use limited to: SHANDONG UNIVERSITY. Downloaded on January 06,2025 at 08:09:21 UTC from IEEE Xplore. Restrictions apply.

This article has been accepted for inclusion in a future issue of this journal. Content is final as presented, with the exception of pagination.

[2] Z. Jiang, W. Zhou, H. Li, Y. Mo, W. Ni, and Q. Huang, "A new kind of accurate calibration method for robotic kinematic parameters based on the extended kalman and particle filter algorithm," *IEEE Trans. Ind. Electron.*, vol. 65, no. 4, pp. 3337–3345, Apr. 2018.

[3] A. Elatta, L. Gen, F. Zhi, Y. Daoyuan, and L. Fei, "An overview of robot calibration," *Inf. Technol. J.*, vol. 3, no. 1, pp. 74–78, 2004.

[4] S. He, L. Ma, C. Yan, C.-H. Lee, and P. Hu, "Multiple location constraints based industrial robot kinematic parameter calibration and accuracy assessment," *Int. J. Adv. Manuf. Technol.*, vol. 102, nos. 5–8, pp. 1037–1050, Jun. 2019.

[5] C. Icli, O. Stepanenko, and I. Bonev, "New method and portable measurement device for the calibration of industrial robots," *Sensors*, vol. 20, no. 20, p. 5919, Jan. 2020.

[6] E. Nieves, N. Xi, B. Du, and Y. Jia, "A reflected laser line approach for industrial robot calibration," in *Proc. IEEE/ASME Int. Conf. Adv. Intell. Mechatronics (AIM)*, Kaohsiung, Taiwan. Piscataway, NJ, USA: IEEE Press, Jul. 2012, pp. 610–615.

[7] P. Yang, Z. Guo, and Y. Kong, "Plane kinematic calibration method for industrial robot based on dynamic measurement of double ball bar," *Precis. Eng.*, vol. 62, pp. 265–272, Mar. 2020.

[8] Y. Liu, D. Shi, and J. Ding, "An automated method to calibrate industrial robot kinematic parameters using Spherical surface constraint approach," in *Proc. 4th Annu. IEEE Int. Conf. Cyber Technol. Automat., Control Intell.*, Hong Kong, China. Piscataway, NJ, USA: IEEE Press, Jun. 2014, pp. 365–370.

[9] Y. Cai, H. Gu, C. Li, and H. Liu, "Easy industrial robot cell coordinates calibration with touch panel," *Robot. Comput.-Integr. Manuf.*, vol. 50, pp. 276–285, Apr. 2018.

[10] D. Bennett and J. Hollerbach, "Autonomous calibration of single-loop closed kinematic chains formed by manipulators with passive endpoint constraints," *IEEE Trans. Robot. Automat.*, vol. 7, no. 5, pp. 597–606, Oct. 1991.

[11] Z. Wang et al., "Field calibration method for industrial robots based on single position sensitive device," *IEEE Trans. Instrum. Meas.*, vol. 72, pp. 1–12, 2023.

[12] J.-H. Borm and C.-H. Meng, "Determination of optimal measurement configurations for robot calibration based on observability measure," *Int. J. Robot. Res.*, vol. 10, no. 1, pp. 51–63, Feb. 1991.

[13] M. R. Driels and U. S. Pathre, "Significance of observation strategy on the design of robot calibration experiments," *J. Robot. Syst.*, vol. 7, no. 2, pp. 197–223, 1990.

[14] A. Nahvi, J. M. Hollerbach, and V. Hayward, "Calibration of a parallel robot using multiple kinematic closed loops," in *Proc. IEEE Int. Conf. Robot. Automat.*, Piscataway, NJ, USA: IEEE Press, 1994, pp. 407–412.

[15] A. Nahvi and J. Hollerbach, "The noise amplification index for optimal pose selection in robot calibration," in *Proc. IEEE Int. Conf. Robot. Automat. Soc.*, Piscataway, NJ, USA: IEEE Press, 1996, pp. 647–654.

[16] Y. Sun and J. M. Hollerbach, "Observability index selection for robot calibration," in *Proc. IEEE Int. Conf. Robot. Automat.*, May 2008, pp. 831–836.

[17] W. Wang, H. Song, Z. Yan, L. Sun, and Z. Du, "A universal index and an improved PSO algorithm for optimal pose selection in kinematic calibration of a novel surgical robot," *Robot. Comput.-Integr. Manuf.*, vol. 50, pp. 90–101, Apr. 2018.

[18] K. Deng, D. Gao, S. Ma, C. Zhao, and Y. Lu, "Elasto-geometrical error and gravity model calibration of an industrial robot using the same optimized configuration set," *Robot. Comput.-Integr. Manuf.*, vol. 83, Oct. 2023, Art. no. 102558.

[19] H. Ye and J. Wu, "Residual index for measurement configuration optimization in robot kinematic calibration," *Sci. China Technol. Sci.*, vol. 66, no. 7, pp. 1899–1915, Jul. 2023.

[20] Y. Wu, A. Klimchik, S. Caro, B. Furet, and A. Pashkevich, "Geometric calibration of industrial robots using enhanced partial pose measurements and design of experiments," *Robot. Comput.-Integr. Manuf.*, vol. 35, pp. 151–168, Oct. 2015.

[21] T. Jiang, H. Cui, X. Cheng, and W. Tian, "A measurement method for robot peg-in-hole prealignment based on combined two-level visual sensors," *IEEE Trans. Instrum. Meas.*, vol. 70, pp. 1–12, 2021.

[22] Z. Yuanfan, T. Wei, and L. Wenhe, "Positional error similarity analysis for error compensation of industrial robots," *Rob. Comput.-Integr. Manuf.*, vol. 42, pp. 113–120, Dec. 2016.



Ziyi Wang (Student Member, IEEE) received the B.E. degree in 2020 in measurement and control technology and instruments from Chongqing University, Chongqing, China, where he is currently working toward the Ph.D. degree in instrument science and technology.

His research interest includes robotic sensing.



Lan Qin received the Ph.D. degree in precision instrument and machinery from Chongqing University, Chongqing, China, in 1994.

Currently, he is a Professor with the College of Optoelectronic Engineering, Chongqing University. His research interests include sensors and actuators, precision measurement of photoelectric sensors, and detection technology and systems.



Jingcheng Liu received the Ph.D. degree in instrument science and technology from Chongqing University, Chongqing, China, in 1994.

Currently, he is a Professor with the College of Optoelectronic Engineering, Chongqing University. His research interests include multiaxis force/acceleration sensor technology and dynamic detection technology.



Min Li received the M.E. degree in precision instrument and machinery from Chongqing University, Chongqing, China, in 1994.

Currently, she is a Professor Level Senior Experimentalist with the College of Optoelectronic Engineering, Chongqing University. Her research interest includes multiaxis force/acceleration sensor calibration technology.



Jun Liu received the Ph.D. degree in instrument science and technology from Chongqing University, Chongqing, China, in 2011.

Currently, he is a Professor with the College of Optoelectronic Engineering, Chongqing University. His research interests include sensor technology and systems, intelligent instrument, and control system.

Authorized licensed use limited to: SHANDONG UNIVERSITY. Downloaded on January 06,2025 at 08:09:21 UTC from IEEE Xplore. Restrictions apply.